A Molecular Study of Pediatric Spindle and Sclerosing Rhabdomyosarcoma

Identification of Novel and Recurrent VGLL2-related Fusions in Infantile Cases

Rita Alaggio, MD, Lei Zhang, MD,† Yun-Shao Sung, MSc,† Shih-Chiang Huang, MD,† Chun-Liang Chen, MSc,† Gianni Bisogno, MD,‡ Angelica Zin, PhD,§ Narasimhan P. Agaram, MD,† Michael P. LaQuaglia, MD,‖ Leonard H. Wexler, MD,¶ and Cristina R. Antonescu, MD†*

Abstract: Sclerosing rhabdomyosarcoma (ScRMS) and spindle cell rhabdomyosarcoma (SRMS) have been recently reclassified as a stand-alone pathologic entity, separate from embryonal RMS. Genetically, a subset of the congenital cases display *NCOA2* gene rearrangements, whereas tumors occurring in older children or adults harbor *MYOD1* gene mutations with or without coexisting *PIK3CA* mutations. Despite these recent advances, a significant number of tumors lack known genetic alterations. In this study we sought to investigate a large group of pediatric SRMS/ScRMS, spanning a diverse clinical and pathologic spectrum, by using a combined fluorescence in situ hybridization, targeted DNA, and whole-transcriptome sequencing methodology for a more definitive molecular classification. A total of 26 SRMS and ScRMS cases were selected from the 2 participating institutions for the molecular analysis. Ten of the 11 congenital/infantile SRMS showed recurrent fusion genes: with novel *VGLL2* rearrangements seen in 7 (63%), including *VGLL2-CITED2* fusion in 4 and *VGLL2-NCOA2* in 2 cases. Three (27%) cases harbored the previously described *NCOA2* gene fusions, including *TEAD1-NCOA2* in 2 and *SRF-NCOA2* in 1. All fusion-positive congenital/infantile SRMS patients with available long-term follow-up were alive and well, none developing distant metastases. Among the remaining 15 SRMS patients older than 1 year, 10 (67%) showed *MYOD1 L122R* mutations, most of them following a fatal outcome despite an aggressive multimodality treatment. All 4 cases harboring coexisting *MYOD1*/*PIK3CA* mutations shared sclerosing morphology. All 5 fusion/mutation-negative SRMS cases presented as intra-abdominal or paratesticular lesions.

Key Words: rhabdomyosarcoma, spindle cell, congenital, *VGLL2*, *SRF*, *TEAD1*, *MYOD1*, *NCOA2*, *CITED2*

(*Am J Surg Pathol* 2016;40:224–235)

Rhabdomyosarcomas (RMSs) are the most common soft tissue sarcomas in children, accounting for 5% to 8% of all pediatric malignancies. Traditionally, RMSs have been divided into 2 clinicopathologic groups: embryonal RMS (ERMS), occurring in younger patients, histologically reminiscent to fetal skeletal muscle, and alveolar RMS (ARMS), often diagnosed in older children, being characterized by a monomorphic round cell cytology, with a variable alveolar pattern and carrying recurrent translocations, a t(2;13)(q35;q14) or t(1;13)(p36;q14) in about 80% of cases.[1] Whereas ARMSs follow a highly aggressive course, the prognosis of ERMS has significantly improved in recent years with an overall survival of 70% at 5 years for patients presenting with localized disease.[2,3]

The spindle cell variant of rhabdomyosarcoma (SRMS) is an uncommon subtype of RMS that was initially grouped under ERMS, having predilection for paratesticular and head and neck sites and being associated with a more favorable behavior in children.[4,5] A subset of SRMSs display areas of prominent hyaline sclerosis and a pseudovascular growth pattern, suggesting morphologic overlap with the even less common sclerosing RMS (ScRMS). ScRMS is characterized by cords or microalveolar patterns, embedded in a prominent sclerotic or hyalinized stroma.[6,7] As both SRMS and ScRMS have similar clinical presentations and overlapping histologic features, it was suggested that they might

From the Departments of *Pathology; ‡Pediatric Hematology-Oncology, University of Padova; §Institute of Pediatric Research Città della Speranza, Padova, Italy; Departments of †Pathology; ‖Surgery; and ¶Pediatrics, Memorial Sloan Kettering Cancer Center, New York, NY.

Conflicts of Interest and Source of Funding: Supported in part by: P50 CA 140146-01 (C.R.A.), Cycle for Survival "Luke's team" (C.R.A., L.W.), Kristen Ann Carr Fund (C.R.A.). The authors have disclosed that they have no significant relationships with, or financial interest in, any commercial companies pertaining to this article.

Correspondence: Cristina R. Antonescu, MD, Department of Pathology, Memorial Sloan Kettering Cancer Center, 1275 York Ave, New York, NY 10065 (e-mail: antonesc@mskcc.org).

Supplemental Digital Content is available for this article. Direct URL citations appear in the printed text and are provided in the HTML and PDF versions of this article on the journal's Website, www.ajsp.com.

represent a morphologic spectrum, with possibly shared pathogenesis.[6,8,9] Subsequently, the latest World Health Organization (WHO) classification merged these 2 entities into a single pathologic entity, distinct from ERMS and ARMS.[10] The recent evidence of recurrent *MYOD1* gene mutations present in both SRMS and ScRMS supports the unifying concept proposed by WHO 2013 on morphologic grounds alone.[11] However, despite these genetic advances and refinement in classification, the heterogeneity of this subgroup of RMS even within the pediatric population has become apparent, as evidenced by important genetic and clinical characteristics being age-dependent. Notably, recurrent *NCOA2* gene rearrangements have been identified in a subset of congenital/infantile SRMS associated with a favorable clinical course.[12] In contrast, all 4 pediatric patients with SRMS/ScRMS carrying *MYOD1* mutations followed a highly aggressive course, similar to the adult patients.[11] In this study we further expand our investigation of pediatric SRMS and ScRMS in a large cohort of different clinical presentations, using a combined molecular approach, including next-generation paired-end RNA sequencing for novel fusion discovery, mutation analysis, and fluorescence in situ hybridization (FISH), for a better molecular subclassification and risk factor stratification in the pediatric age group.

MATERIALS AND METHODS

Patient Selection

Archival material from pediatric patients with diagnosis of SRMS or ScRMS was retrieved from the Institutional and consultation files of the Departments of Pathology of the University of Padua and Memorial Sloan Kettering Cancer Center. Twenty-six cases were identified, and the diagnosis was confirmed on the basis of histologic features and positive immunohistochemical reactivity for desmin and myogenin. All cases were screened at diagnosis for *PAX3/7-FOXO1* gene fusions either by reverse transcription polymerase chain reaction (RT-PCR) or FISH and were negative. All cases had archival formalin-fixed paraffin-embedded material for further molecular testing. In addition, 6 cases had adequate frozen tissue material, 4 of these being subjected to paired-end RNA sequencing, and 2 were previously analyzed by 5′RACE.[12] Three cases were previously included in the study by Mosquera et al[12] and 4 cases by Agaram et al[11] (Table 1). The study was approved by the Institutional Review Board at each institution.

Clinicopathologic Features

The clinical data of the 26 patients (11 boys and 15 girls) with an overall age range of 0 to 17 years (median 3 y, mean 5.5 y) are summarized in Table 1. Eleven of these patients were diagnosed at birth (congenital) or within 1 year of age (infantile), with equal sex distribution. All except 1 of the congenital/infantile cases were located in the trunk: back/paravertebral areas, 5; chest wall, 3; posterior neck/paraspinal, 2. Only 1 occurred in the limb soft tissues (calf). The remaining 15 patients, 9 boys and 6 girls, were diagnosed in older children, with a mean age of 9.4 years (range 2 to 17 y, median 9.5 y). The anatomic distribution for this latter subgroup was more variable, with 5 intra-abdominal/paratesticular, 3 cases in the trunk (paraspinal, paravertebral, back), 4 in the head and neck (infratemporal, cheek, orbit), 2 in the buttock, and 1 in the thigh.

Hematoxylin and eosin–stained slides from all cases were reviewed by 2 sarcoma pathologists (R.A., C.R.A.). The diagnosis of SRMS was defined according to the current criteria proposed by WHO 2013 classification, when there was a predominant spindle cell morphology, with only focal if any rhabdomyoblastic differentiation and absent or minimal nuclear pleomorphism. ScRMS was defined as tumors with variable cellularity, composed of spindle cells or round cells arranged in a pseudovascular/pseudoalveolar or tubular-like pattern, embedded in a hyalinizing stroma. Positive immunostaining for desmin and, at least focally, for myogenin were required for diagnosis.

A detailed morphologic examination was carried out in each case, recording the predominant growth pattern (herring-bone, fascicular, fibromatosis-like), amount and quality of cytoplasm, degree of cytologic atypia (nuclear hyperchromasia, type of chromatin degree of nuclear pleomorphism), mitotic rate, and type of stromal component. On the basis of some of these features the tumors were also defined as resembling other mesenchymal tumors, such as fibrosarcoma-like, leiomyosarcoma-like, and fibromatosis-like. Clinicopathologic features, including size, location, management, and follow-up, were obtained from the medical records for all cases. Subsequently, the histologic features were compared with the results of cytogenetic and molecular characterization.

RNA Sequencing

Four cases were analyzed by RNA sequencing (SRMS #1, 6, 7, 17). Total RNA was prepared for RNA sequencing in accordance with the standard Illumina mRNA sample preparation protocol (Illumina). Briefly, mRNA was isolated with oligo(dT) magnetic beads from total RNA (2 μg). The mRNA was fragmented by incubation at 94°C for 2.5 minutes in fragmentation buffer (Illumina). To reduce the inclusion of artifact chimeric transcripts into the sequencing library, an additional gel size–selection step was introduced before the adapter ligation step.[13] The adaptor-ligated library was then enriched by PCR for 15 cycles and purified. The library was sized and quantified using DNA1000 kit (Agilent) on an Agilent 2100 Bioanalyzer according to the manufacturer's instructions. Paired-end RNA sequencing at read lengths of 50 or 51 bp was performed with the HiSeq 2000 (Illumina). A total of about 60.9 million paired-end reads were generated, corresponding to about 3.1 billion bases.

Analysis of RNA Sequencing Results With FusionSeq and TopHat

All reads were independently aligned with the STAR (ver 2.3)[14] and TopHat2 (ver 2.0.14)[15] against the

TABLE 1. Clinicopathologic and Molecular Features of Pediatric SRMS/ScRMS

RMS#	Age/Sex	Site	Diagnosis	Molecular Results	FU (y)	IRS	Status
1*	0.7/M	Post-neck	SRMS	SRF-NCOA2†	3	I	NED, CR2
2*	4W/M	Chest wall	SRMS	TEAD1-NCOA2	3	IIa	NED
3*,‡	0.3/F	Chest wall	SRMS	VGLL2-NCOA2	13	III	NED, CR4
4	0/M	Calf	SRMS	TEAD1-NCOA2	NA	NA	NA
5	0.2/F	Back	SRMS	VGLL2-NCOA2	NA	NA	NA
6	0/F	Back	SRMS	VGLL2-CITED2†	9	III	NED, CR
7	0/F	Back	SRMS	VGLL2-CITED2†	6	III	NED, CR
8	0.7/F	Back	SRMS	VGLL2-CITED2	8	II	NED, CR
9	0/F	Lower neck/back	SRMS	VGLL2-CITED2	Recent case	I	In therapy
10	0.8/M	Chest wall	SRMS	VGLL2	NA	NA	NA
11	0.4/M	Paravertebral	SRMS	—	NA	NA	NA
12§	10/F	Paraspinal	SRMS	MyoD1 (L122R)‖	3	III	DOD
13§	2/F	Buttock	SRMS	MyoD1 (L122R)	1	IIa	DOD
14	17/M	Paravertebral	ScRMS	MyoD1 (L122R)‖	2	III	DOD
15§	15/F	Infratemporal	ScRMS	MyoD1 (L122R)‖,¶	1	III	DOD
16§	13/F	Back	ScRMS	MyoD1 (L122R)‖,¶	2	III	DOD
17	10/F	Buttock	ScRMS	MyoD1 (L122R) ¶,† FGFR4 (V548M)	0.5	III	DOD
18	8/M	Thigh	ScRMS	MyoD1 (L122R)‖	1	III	NED, CR1
19	11/F	H&N	ScRMS	MyoD1 (L122R)‖,¶	Recent case	I	In therapy
20	9/M	H&N	SRMS	MyoD1 (L122R)‖	3	III	AWD (2nd LR)
21	9/F	H&N	SRMS	MyoD1 (L122R)‖	1	III	DOD
22	3/M	Intra-abd	SRMS	—	13	I	NED, CR2
23	16/M	Paratesticular	SRMS	—	1	I	NED, CR
24	5/F	Intra-abd	SRMS	FGFR4 (V550L)	NA	NA	NA
25	2.8/F	Ovary/salpinx	SRMS	—	2	III	DOD
26	11/M	Paratesticular	ScRMS	—	1	II	NED, CR

IRS, according to the Intergroup Rhabdomyosarcoma Study Group pretreatment staging classification.
*Included in Mosquera et al.[12]
†Cases tested by RNAseq.
‡Case tested by 5′-RACE.
§Included in Agaram et al.[11]
‖Homozygous MyoD1 (L122R) mutations.
¶Coexisting PIK3CA mutations.
AWD indicates alive with disease; CR, complete remission; DOD, dead of disease; F, female; FU, follow-up; H&N, head and neck; intra-abd, intra-abdominal; LR, local recurrence; M, male; NA, not available; NED, no evidence of disease; Tx, therapy.

human reference genome (hg19), followed by FusionSeq[16] and TopHat Fusion (ver 0.1.0),[17] respectively, to identify fusion candidates. In the first analysis, mapped reads were converted into Mapped Read Format[18] and analyzed with FusionSeq to identify potential fusion transcripts. An *SRF-NCOA2* fusion candidate was identified by FusionSeq in SRMS1 and experimentally validated as previously reported.[12] However, for the additional 3 new cases (SRMS #6, 7, 16) no fusion candidates were identified with this pipeline. We then applied TopHat fusion analysis tool to detect potential gene fusion events with spanning reads >20 bp. In contrast to FusionSeq, TopHat fusion aligns reads without relying on existing annotation and directly detects individual reads that span the fusion event. This tool proved to be more sensitive to detect small intrachromosomal inversions, which most likely were filtered out by the FusionSeq algorithm. In addition, RNAseq data were analyzed for gene mutation calls. BAM files were generated by STAR alignment, followed by PicardTools (ver 1.130) standard preprocessing, which include marking of duplicate reads, recalibration of base quality scores, and local realignment. MuTect (var 1.15)[19] and VarScan (var 2.3.8)[20] variant callers were both applied for mutation detection, followed by vcf2maf (https://github.com/ckandoth/vcf2maf) for converting VCF into MAF files, with the annotation added by Variant Effect Predictor tool provided by Ensembl. (http://useast.ensembl.org/info/docs/tools/vep/index.html). Variants with missense and frameshift mutation in the 340 genes from the IMPACT panel were considered, and potential mutation locations were compared with NCBI dbSNP (http://www.ncbi.nlm.nih.gov/snp), cBioPortal (http://www.cbioportal.org/), and COSMIC (http://cancer.sanger.ac.uk/cosmic). Sanger PCR validation was performed subsequently.

Fluorescence In Situ Hybridization

FISH on interphase nuclei from paraffin-embedded 4-μm-thick sections was performed applying custom probes using bacterial artificial chromosomes (BAC), covering and flanking *VGLL2, CITED2, NCOA2, SRF,* and *TEAD1* (Supplementary Table 1, Supplemental Digital Content 1, http://links.lww.com/PAS/A317). BAC clones were chosen according to UCSC genome browser (http://genome.ucsc.edu) and obtained from BAC-PAC sources of Children's Hospital of Oakland Research Institute (CHORI; Oakland, CA; http://bacpac.

chori.org). DNA from individual BACs was isolated according to the manufacturer's instructions, labeled with different fluorochromes in a nick translation reaction, denatured, and hybridized to pretreated slides. Slides were then incubated, washed, and mounted with DAPI in an antifade solution. The genomic location of each BAC set was verified by hybridizing them to normal metaphase chromosomes. Two hundred successive nuclei were examined using a Zeiss fluorescence microscope (Zeiss Axioplan, Oberkochen, Germany), controlled by Isis 5 software (Metasystems). A positive score was interpreted when at least 20% of the nuclei showed a break-apart signal. Nuclei with incomplete set of signals were omitted from the score.

Targeted PCR and Sanger Sequencing

Genomic DNA was isolated either from fresh-frozen or archival paraffin tissue, as described previously[21] in all fusion-negative samples. Targeted PCR was performed for the known *MYOD1* exon 1 hotspot mutation and *PIK3CA* exons 9 and 20 mutations as previously reported.[11] Direct sequencing of PCR products was performed and compared with the NCBI human *MYOD1* and *PIK3CA* gene sequences. For the FGFR4 kinase domain validation we used the following primers: *FGFR4* exon 13 Fwd: 5′-CAATGTCCCGAC
TTCTCCCTCTC-3′ and *FGFR4* exon 13 Rev 5′-CAG GTTGATGATGTTCTTGTGTCG-3.

RT-PCR Validation and 5′RACE

The *VGLL2-CITED2* fusion candidate identified by TopHat fusion was validated by RT-PCR using 1 μg of total RNA and cDNA synthesis by SuperScript III First-Strand Synthesis Kit (Invitrogen, Carlsbad, CA). RT-PCR was performed using the advantage 2 PCR kit (Clonetech, Mountain View, CA) for 33 cycles at a 65°C annealing temperature, using the following primers: *VGLL2* Intron 3 fwd 5′-GTCTGCCCACTGCCCCTTTC-3′; *CITED2* Ex2 rev 5′-GGTTGAAATACTGGTTGTTGAGC-3′. The PCR product was confirmed by agarose gel electrophoresis and then sequenced using the Sanger method.

5′RACE was performed in SRMS3 using the SMARTer RACE cDNA Amplification Kit (Clonetech). Reverse transcribed mRNA was initiated by SMARTer II A Oligonucleotide with appropriate 5′-RACE CDS Primer A in a 10 μL reaction volume according to the manufacturer's protocol. Primary PCR was performed by Advantage 2 polymerase chain reaction (Clonetech) with the SMARTer RACE Universal Primer A Mix and reverse primer on *NCOA2* exon 15 (5′-TCCTCCAAAT-CAGACTGCCCCAT-3′). Nested PCR was performed with the SMARTer RACE Nested Universal Primer A and reverse primer on *NCOA2* exon 14 (5′- GGAACC-CAGCAGCCAGCATC -3′). Amplified PCR products were being cloned by TOPO TA Cloning Kit for Sequencing with One Shot TOP10 Chemically Competent *E. coli* (Invitrogen). The constructed plasmid DNA was sequenced using the Sanger method.

Western Blotting

Frozen tissue from the 2 samples with *VGLL2-CITED2* fusions (SRMS6, SRMS7) and 1 control sample (normal skeletal muscle) were homogenized in Tissue Protein Extraction Reagent (Thermo Scientific, Cat# 78510) supplemented with protease inhibitors. Electrophoresis and immunoblotting were performed on the protein extracts using 30 μg of protein per sample. VGLL2 and β-Actin expression were detected by anti-VGLL2 mouse polyclonal antibody (Abcam, Cat# ab169247) with 1:500 dilution and anti-Actin mouse monoclonal antibody (Cell Signaling, Cat#3700) with 1:1000 dilution, respectively. Following hybridization with the secondary rabbit anti-mouse antibody (Santa Cruz Biotechnology, Santa Cruz, CA; #sc-358923) with 1:5000 dilution, the blots were incubated with Immun-Star horseradish peroxidase luminal/enhancer (Bio-Rad, Hercules, CA) and exposed onto Kodak Biomax MR Film (Eastman Kodak Co., Rochester, NY).

RESULTS

Congenital/Infantile SRMSs Show Recurrent Gene Fusions, Involving VGLL2, SRF, and TEAD1, Critical Transcriptional Regulators of Skeletal Muscle Function

Two of the 3 infantile SRMS tested by TopHat Fusion algorithm showed similar *VGLL2-CITED2* gene fusion candidates (SRMS6, SRMS7), which resulted from an intrachromosomal 6 inversion, as the 2 genes have opposite directions of transcription (Fig. 1A). RT-PCR confirmed the fusion of *VGLL2* intron 3 with *CITED2* exon 2 (Fig. 1B). FISH studies further validated this result in both cases (Fig. 1C). All the remaining cases were further tested by FISH for *VGLL2* gene abnormalities, and 5 additional cases were found to have *VGLL2* break/inversion. These 5 cases were further investigated for potential partners and confirmed 2 additional cases with *VGLL2-CITED2* fusion (SRMS8, SRMS9), 2 with *VGLL2-NCOA2* (SRMS3, SRMS5), and 1 without an identifiable partner (SRMS10). SRMS3 was previously reported by our group as having an *NCOA2* gene rearrangement without a proven gene partner.[12] Repeat 5′RACE analysis on this case showed the fusion of *VGLL2* exon 2 with *NCOA2* exon 14 (Fig. 2), this result being further confirmed by FISH (Fig. 2). The remaining 3 cases showed *SRF-NCOA2* fusions in 1 case (SRMS1) and *TEAD1-NCOA2* (SRMS2, SRMS4) in 2 cases.[12] Only 1 tumor (SRMS11) in this group was not associated with gene fusion abnormalities.

Histologically, all 10 fusion-positive infantile SRMS showed a striking resemblance with infantile fibrosarcoma (Fig. 3), with no morphologic differences among the different fusion types. The lesional cells were monomorphic, with delicate, scant eosinophilic cytoplasm and oval to wavy nuclei, with finely dispersed chromatin, and occasional, inconspicuous nucleoli (Figs. 3A–C). Hyperchromasia was seen in 2 cases as focal and in 1 case as more diffuse (Figs. 3D–H). Alternating hypocellular areas were present in 4 cases, with collagen bundles interspersed

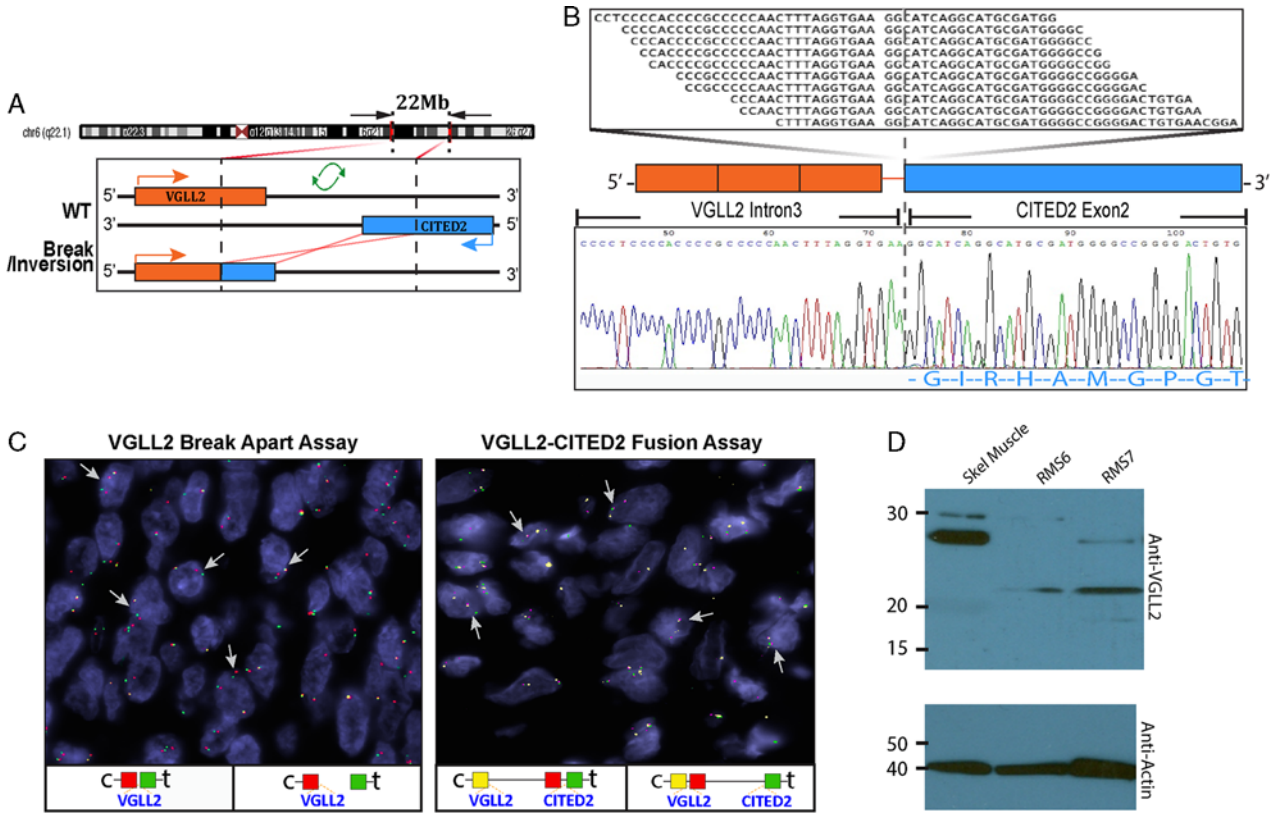

FIGURE 1. Novel *VGLL2-CITED2* fusion gene discovery in congenital/infantile SRMS by RNA sequencing and TopHat-seq data analysis. A, Diagrammatic representation of the 6q22-q23 region breaks at the *VGLL2* and *CITED2* loci, followed by an inversion and fusion of the 3′*CITED2* to the 5′*VGLL2* portion. B, Fusion candidates were validated by RT-PCR showing fusion of the 1020 bp of *VGLL2* intron 3 to *CITED2* exon 2 (SRMS6). C, FISH validation of *VGLL2-CITED2* fusion, first by the *VGLL2* break-apart assay (left panel) (arrows show constant split signal, in keeping with an intrachromosomal inversion/break; red, centromeric; green, telomeric) and followed by the *VGLL2-CITED2* 3-color fusion assay (right panel) (arrows show red-yellow fused signals; red, centromeric of *CITED2*; yellow, *VGLL2*). D, Western blotting showing lack of the 28 kDa wild-type VGLL2 band in the 2 *VGLL2-CITED2* fusion-positive cases (SRMS6 and SRMS7) compared with the control skeletal muscle. Instead, they show a lower band, possibly truncated protein at 22 kDa molecular weight.

between cells, reminiscent of a desmoid-type fibromatosis (Fig. 3I). There was no evidence of necrosis. The mitotic rate was typically <5 mitoses/10 HPF, except for SRMS2 with >10/10 HPF. One case (SRMS10) displayed unusual myoid features with a vaguely perivascular pattern of arrangement, mimicking a myofibromatosis. The only fusion-negative tumor, occurring in a 4-month-old baby (SRMS11), showed a more conventional SRMS morphology, characterized by elongated cells with more abundant eosinophilic cytoplasm, scattered large hyperchromatic nuclei, and >10/10 HPF. All tumors showed patchy to diffuse desmin reactivity and scattered, multifocal myogenin and MyoD1 reactivity.

MYOD1-positive S/ScRMSs Occur in Older Children With Predilection in the Trunk and Head and Neck

Among the 15 SRMSs occurring in older children, 10 (67%) had *MYOD1 L122R* exon 1 mutations, as detected by Sanger sequencing. In all except 2 cases there were *MYOD1 L122R* homozygous mutations (Table 1); both heterozygous *MYOD1*-mutant cases occurred in female individuals and in the buttock location (2-y-old and 10-y-old). Four of these *MYOD1*-mutant cases harbored coexisting *PIK3CA* mutations, 3 being in the exon 10 helical domain (*E542V, E545K,* and *Q546R)* and 1 in the exon 21 kinase domain (*G1049R*). The latter case had available frozen tissue (RMS17) and was studied by RNAseq as initially being diagnosed as an unclassified RMS (possibly representing a fusion-negative solid ARMS). As the TopHat algorithm did not identify any fusion candidates, it was further subjected to mutation detection algorithms, which identified *MYOD1 L122R*, *PIK3CA G1049R,* and *FGFR4 V548M* mutations. These mutations were then confirmed by Sanger sequencing. Upon morphologic re-review, the tumor showed focal areas of sclerosis intermixed within the mostly solid round cell component (Fig. 5); thus the case was reclassified as a cellular variant of ScRMS supported by the above mutational profile. In fact all cases with coexisting *MYOD1* and *PIK3CA* mutations were associated with sclerosing histology, being composed of variably cellular, but monomorphic, round to spindle cells embedded in a distinctive

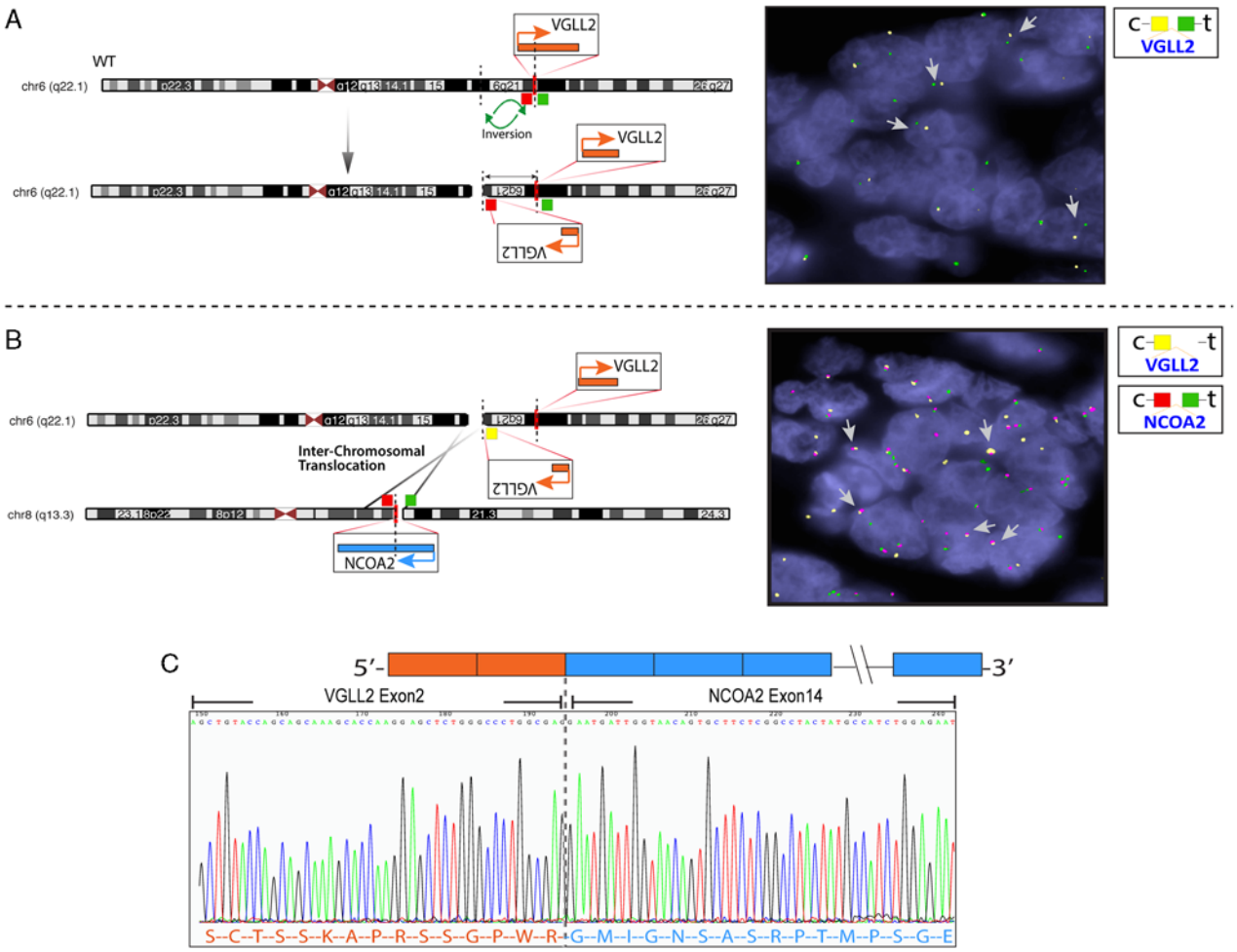

FIGURE 2. Novel *VGLL2-NCOA2* complex fusion in congenital/infantile SRMS by 5′RACE. As *VGLL2* and *NCOA2* genes have opposite directions of transcription, a functional fusion requires a break/inversion of one of the partners. A, Schematic view of the intragenic *VGLL2* break and inversion, confirmed by *VGLL2* break-apart FISH with constant split signals (yellow, centromeric; green, telomeric). B, Schematic diagram of the t(6;8) translocation, fusing the 5′*VGLL2* portion to the 3′*NCOA2*; subsequent FISH validation using 3-color *VGLL2-NCOA2* fusion assay (arrows showing fused red-yellow signals; yellow, centromeric of *VGLL2*; red, centromeric of *NCOA2*). C, 5′RACE showing the fusion of *VGLL2* exon 2 to *NCOA2* exon 14 (SRMS3).

hyalinized stroma. The remaining *MYOD1*-mutant SRMSs displayed a classic morphology, composed of intersecting long fascicles of elongated cells with scant to moderate amount of fibrillary eosinophilic cytoplasms and uniform oval nuclei, reminiscent of leiomyosarcoma (Fig. 5). Rhabdomyoblastic differentiation, although very focal, was often present in the form of scattered rhabdomyoblasts intermixed among the spindle cells. Patchy hyperchromasia was also present, with mostly scattered cytologic atypia. Three tumors showed increased mitotic activity of >10 MF/10 HPF and geographic necrosis.

The remaining 5 cases lacking both fusions and *MYOD1* mutations showed overlapping morphologic features with the *MYOD1*-mutant SRMS (Supplementary Fig. 1, Supplemental Digital Content 2, http://links.lww.com/PAS/A318). In addition, 2 of the cases showed focal myxoid areas. Two cases showed an increased mitotic rate of >10 MF/10 HPF. All cases showed mostly diffuse positivity for desmin, whereas myogenin nuclear staining was found ranging from 5% to 50% of the cells. Additional targeted DNA PCR for the *FGFR4* hotspot mutations showed the presence of an *FGFR4* exon 13 *V550L* in SRMS24 (Table 1).

Fusion-positive Infantile SRMSs Follow a Favorable Clinical Course Compared With the Highly Aggressive Behavior of Older Children With SRMS Harboring MYOD1 Mutations

All patients were treated with preoperative chemotherapy after the diagnosis of SRMS or ScRMS was rendered on the biopsy, except for the 2 paratesticular tumors, which were treated with surgery and subsequent chemotherapy. All 6 fusion-positive congenital/infantile SRMS patients with available long-term follow-up are presently alive and well after a median of 7 years (range, 3 to 13 y). Two patients developed local recurrences, but

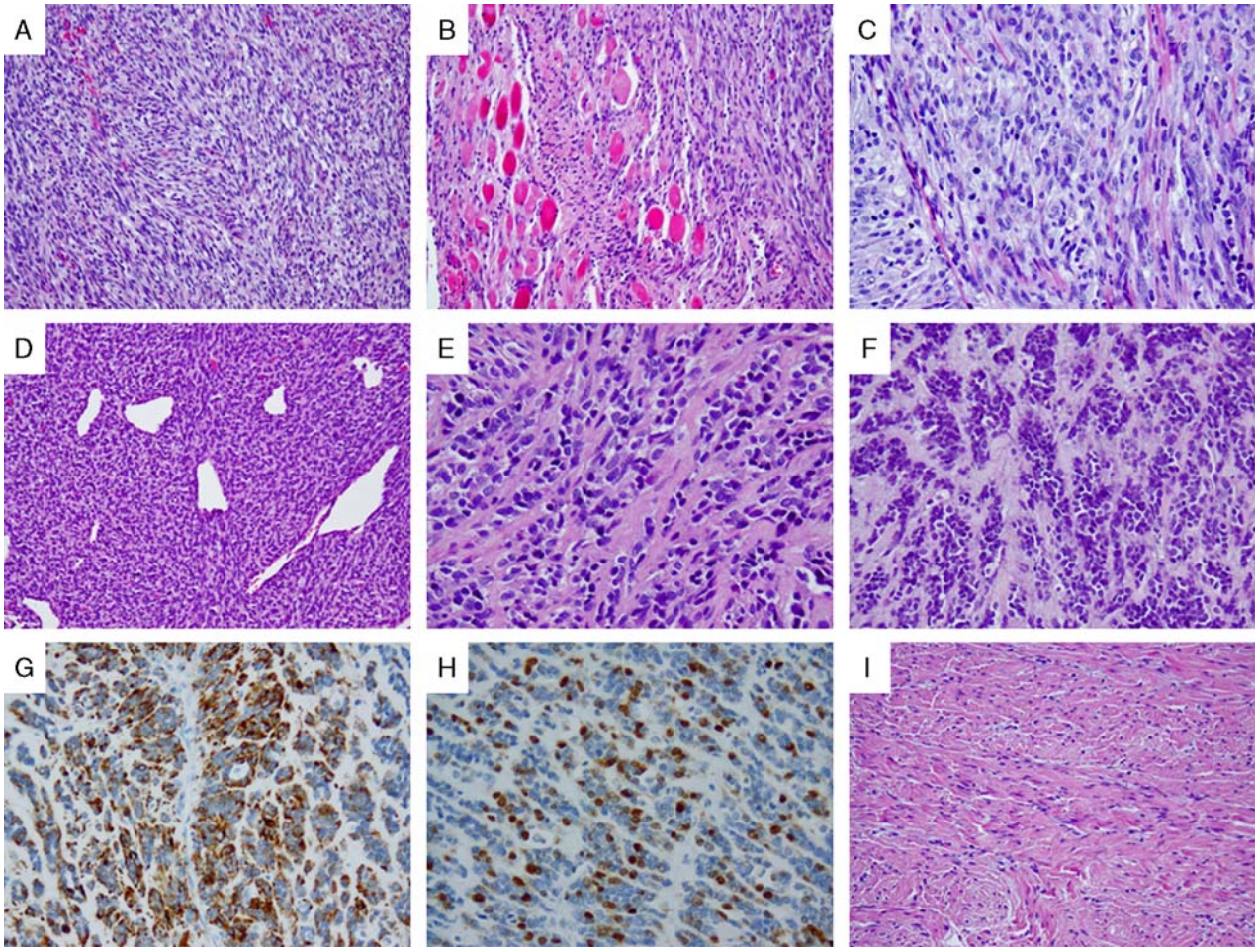

FIGURE 3. Pathologic features of congenital/infantile fusion-positive SRMS. *VGLL2-CITED2* fusion-positive tumors shared similar morphology (A–C) with monomorphic spindle cells arranged in short intersecting fascicles (A, SRMS6), infiltrating within skeletal muscle (B, SRMS6) and showing a more plump oval cells with pale eosinophilic to clear cytoplasm, fine chromatin, and scattered mitotic figures (C, SRMS7). *VGLL2-NCOA2* fusion-positive tumor (SRMS3) showed a highly cellular and hyperchromatic appearance reminiscent of infantile fibrosarcoma with a distinctive hemangiopericytoma-like vascular pattern in the primary tumor (D); in the subsequent 2 local recurrences, 2 years (E) and 5 years (F) later, it had a more sclerosing appearance; latter recurrence showed reactivity for desmin (G) and myogenin (H). In contrast, a *VGLL2* rearranged tumor with no identifiable partner showed a more sclerotic background mimicking fibromatosis (SRMS10, I).

none developed distant metastases. In contrast, 7 of the 9 *MYOD1*-mutant RMS patients died of disease, including the 3 cases with sclerosing morphology and coexisting *MYOD1*/*PIK3CA* mutations, with a median of 1.5 years (range, 1 to 3 y). Only 1 patient in this group is alive and well after only 1 year of follow-up, and an additional patient is alive with disease after developing a second local recurrence. Among the fusion/*MYOD1* mutation–negative subset, 3 of the 4 cases with available follow-up are with no evidence of disease, including the 2 patients with paratesticular and 1 with paraovarian tumors.

DISCUSSION

Despite a relatively homogenous morphologic phenotype, SRMS has emerged as a diverse group of tumors, with different molecular genetic profiles and variable clinical behaviors depending on the age at presentation. In the pediatric population, SRMS was first described by Cavazzana et al[4] in 1992 and subsequently by Leuschner et al[5] a year later as a variant of ERMS, typically occurring in the paratesticular or head and neck region, with histologic features mimicking a leiomyosarcoma. Their clinical behavior appeared to be more favorable compared with classic ERMS. In contrast, Lundgren et al[22] described a small series of 3 SRMSs occurring in children aged 1 to 3 years and displaying a morphology reminiscent of infantile fibrosarcomas (infantile rhabdomyofibrosarcomas), but followed a fatal course in 2 cases. Moreover, in adults, SRMSs also have a predilection for the head and neck region but, unlike the pediatric tumors, seem to follow a more aggressive clinical course.[8,23,24] As the evidence for SRMS having distinct clinicopathologic features from ERMS and sharing morphologic features

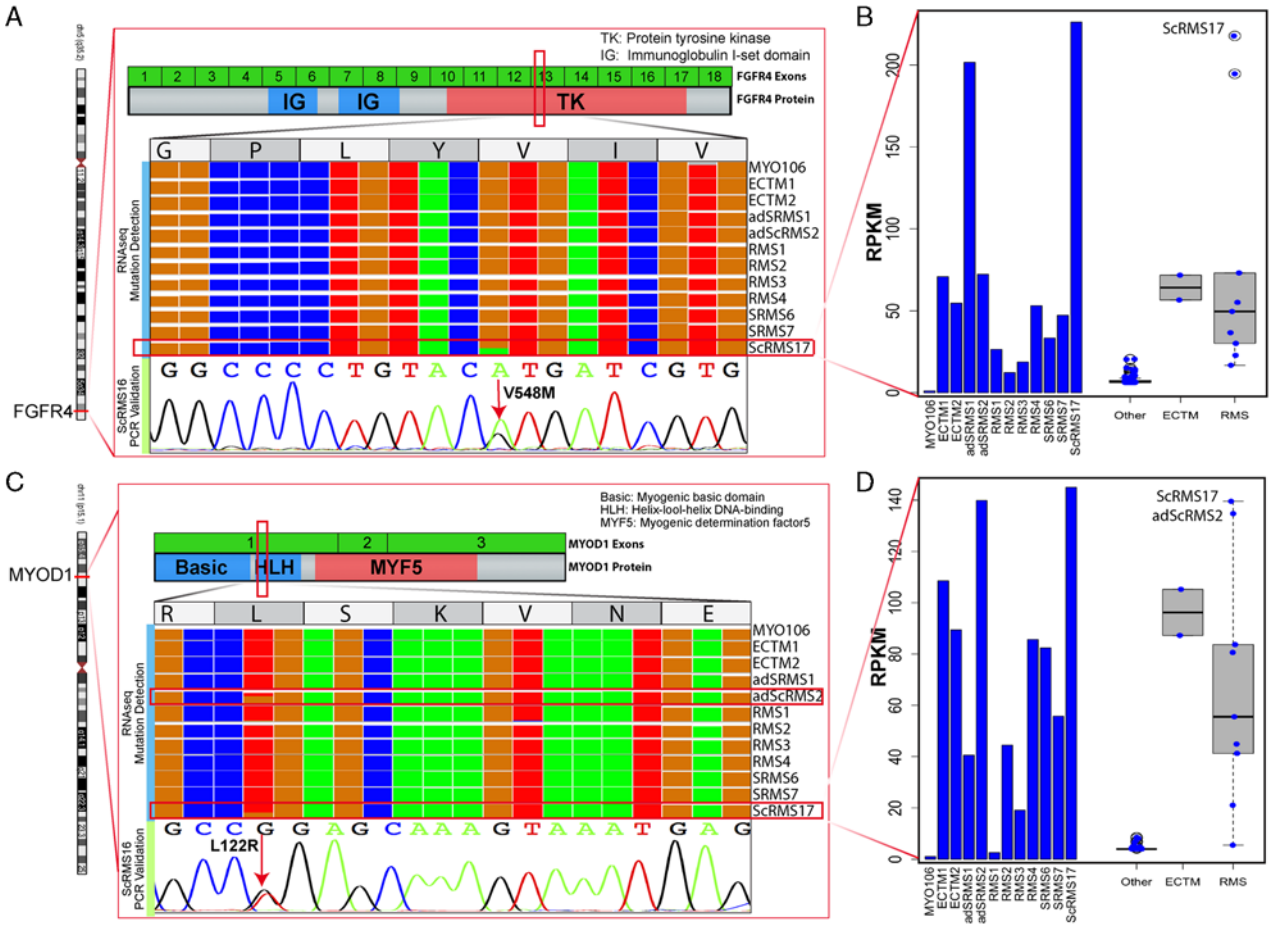

FIGURE 4. Novel *FGFR4* kinase domain mutation in a poorly differentiated ScRMS with coexisting *MYOD1* and *PIK3CA* mutations. A, IGV (integrated genomic viewer) tool using RNAseq data showing *FGFR4* kinase domain mutation at the V548 position (exon 13) with a 49% allelic frequency and read coverage of 717 in SRMS17, compared with other RMS cases. B, Bar chart showing high *FGFR4* mRNA expression in ScRMS17, compared with other tumor types and RMS cases (including SRMS6 and SRMS7 with *VGLL2-CITED2* fusions; 2 ectomesenchymomas [ECTM], 1 infantile myofibroma [MYO1], and other subtypes of RMS). Of note, similarly high *FGFR4* expression was seen in an adult SRMS, lacking *MYOD1*, *PIK3CA*, and *FGFR4* mutation (adSRMS1). C, IGV showing *MYOD1 L122R* mutation with a 42% allele fraction and read coverage of 883 and further confirmed by Sanger sequencing as a heterozygous mutation. D, Bar chart showing overall high expression of *MYOD1* mRNA across different RMS and ectomesenchymomas compared with other tumor types, with highest levels in the 2 cases harboring *MYOD1* mutations (adSRMS2, SRMS17).

with ScRMS became more widely accepted, it led to its reclassification in the latest WHO classification as a stand-alone pathologic entity.[10]

From the genetic viewpoint, we have previously described recurrent *NCOA2* gene rearrangements in a small subset of SRMS occurring in the infantile/congenital setting.[12] As *NCOA2*-related fusions were only seen in infants, we speculated that SRMS/ScRMS represents a heterogenous genetic group of tumors among different age groups. Notably, all 3 *NCOA2*-rearranged SRMSs pursued a favorable clinical course and lacked metastatic potential. The additional 7 fusion-positive infantile SRMSs reported here reinforce our initial results of a very favorable outcome, all patients being without evidence of disease after long-term follow-up.

Herein, we identify novel *VGLL2* gene rearrangements located at the 6q22 locus as the most common (64%) genetic abnormality in congenital/infantile SRMS, being fused to either *NCOA2* or *CITED2* gene partners. This result is not so surprising as VGLL2 is expressed in differentiating somites and branchial arches during embryogenesis and is exclusively expressed in skeletal muscle in the adult.[25] VGLL2 (Vestigial-like 2, a.k.a. VGL2 or VITO1) was identified as a human homolog of a Drosophila protein, Vestigial, a transcriptional coactivator (without DNA-binding sequence) of Scalloped, that contains the TEA domain and is required for wing formation.[26,27] VGLL2 is a key cofactor of TEF-1 (transcription enhancer factor-1, a.k.a. TEAD1) and MEF2 (myocyte enhancer factor-2) family members regulating

muscle-specific gene transcription in skeletal muscle[25,28] (Supplementary Fig. 2, Supplemental Digital Content 3, http://links.lww.com/PAS/A319). In Drosophila, Vgl2 plays a key role in the development and patterning of the wing: its loss results in a failure of wing development, whereas its overexpression leads to the development of ectopic wings.[29] In humans, upon muscle differentiation VGLL2 is upregulated and translocates from the cytoplasm to the nucleus, where it interacts with MEF2 and coactivates TEF-1 and MEF2-dependent muscle-specific promoters. Although VGLL2 alone is not sufficient to initiate myogenic conversion of 10T1/2 fibroblasts in vitro, it enhanced MyoD-mediated myogenic conversion, suggesting that it is a crucial cofactor of the muscle regulatory program.[30]

Our results thus implicate a number of critical transcription factors or coactivators involved in skeletal muscle function in the pathogenesis of congenital/infantile SRMS. As most of these cases do not show overt rhabdomyoblastic differentiation morphologically and sometimes display only patchy desmin reactivity, it is intriguing to speculate that their oncogenic role in this tumor is to block skeletal muscle differentiation and maintain a primitive phenotype. Both SRF (serum response factor) and TEAD1 (TEA domain, a.k.a. TEF-1) have been shown to be involved in the control of muscle-specific gene transcription. SRF is highly expressed in skeletal muscle and controls the expression of genes specifically expressed in skeletal muscle (*dystrophin, muscle creatine kinase, myoD*), including several genes encoding sarcomeric proteins (such as *α skeletal actin, myosin light chain, tropomyosin*).[31] TEAD1 is constitutively expressed in cardiac and skeletal muscle, acting as a key molecule of muscle development, transactivating multiple target genes involved in cell proliferation and differentiation pathways.[32]

In the context of SRMS, these muscle-specific factors (VGLL2, SRF, TEAD1) participate as 5′ partners in the recurrent translocations and maintain most of their key functional domains within the fusion protein. Thus VGLL2 retains its vestigial motif (Vg), SRF preserves the MADS box and TEAD1 its TEA domain (Supplementary Fig 2, Supplemental Digital Content 3, http://links.lww.com/PAS/A319). Interestingly, our RNA sequencing showed that the *VGLL2-CITED2* fusion product contained a large intronic sequence of *VGLL2* intron 3, which most likely results in a truncated protein. This result is further confirmed by our Western blotting, showing lack of a wild-type VGLL2 protein, compared with normal skeletal muscle, in keeping with a loss of function effect (Fig. 1). *VGLL2* 3′ fusion partners are either *NCOA2* on 8q13.3 or *CITED2* on 6q23.3. The exact role of these genes within the fusion remains unclear, as no upregulation of either *VGLL2* or *CITED2* was noted in the 2 cases with available RNAseq data, suggesting a different role of the fusion transcript other than gene overexpression. CITED2 (Cbp/p300-interacting transactivator with Glu-Asp-rich carboxy-terminal domain, 2) is a cardiac transcription factor, which is essential for heart development.[33] CITED2-deficient mice show cardiac malformations, adrenal agenesis, and neural crest defects. Mutations in this gene were reported to cause cardiac septal defects.[34] Of interest, fusions involving the *CITED2* gene have been described recently in a case of high-grade undifferentiated pleomorphic sarcoma, the gene, however, being the 5′ partner and fused to *PRDM10* on 11q24.[35] CITED2 is a nuclear protein that binds closely to the CH1 region of p300 and CBP. In contrast, NCOA2 (nuclear receptor coactivator) is a member of the p160 steroid receptor coactivator gene family. In the COOH-terminal part of NCOA2 there are 2 intrinsic transcriptional activation domains, TAD1 and TAD2,[36,37] which are responsible for interaction with general transcriptional cointegrators such as CBP and p300. This is intriguing as both CITED2 and NCOA2 maintain their carboxy-terminal in the projected fusion protein structure, thus sharing a CBP/p300 interaction domain, which may be involved in the pathogenesis of SRMS (Supplementary Fig. 2, Supplemental Digital Content 3, http://links.lww.com/PAS/A319).

SRMSs harboring *MYOD1* mutations were first described in the adult population, in about 44% of cases tested.[38] Our group subsequently reported their occurrence in both pediatric age group and in sclerosing morphology.[11] In our initial study, all the 4 pediatric *MYOD1*-mutated RMS patients died of the disease at 2-year median follow-up. Interestingly, 2 of the 4 cases showing coexisting *PIK3CA* helical mutations were associated with sclerosing morphology.[11] Of interest, *MYOD1* mutations were also reported in 10% of ERMS,[39] albeit described as having mostly a spindle cell morphology. However, *MYOD1* mutations were not identified in a large genomic study encompassing both fusion-positive ARMS and fusion-negative ERMS.[40] In our expanded cohort of 9 *MYOD1*-mutant SRMSs, we confirm the initial observations that this genotype is seen in older children (mean age, 10 y), presenting with predilection in the trunk and head and neck area. The presence of *MYOD1* mutations is associated with a highly aggressive course despite multimodality treatment, with 7/9 children with available follow-up dying of disease within 1 year of diagnosis. Once again the coexisting *PIK3CA* mutation was associated with sclerosing morphology. Of note, 1 of the ScRMSs tested by RNAseq showed 3 coexisting mutations: *MYOD1 L122R*, kinase domain *PIK3CA G1049R*, and kinase domain *FGFR4 V548M*. Although previous kinase domain mutations in *FGFR4* have been reported in about 6% to 7% of RMS,[40,41] mostly in ERMS,[42] this case appears to be the first report of *FGFR4* mutations in an SRMS/ScRMS. The RNAseq in this case showed high upregulation of *FGRF4* mRNA (Fig. 4). Furthermore, the association of these 3 activating mutations in 1 single case might explain the highly undifferentiated phenotype noted, reminiscent of a fusion-negative solid ARMS. Only in retrospect, after the mutation profile became available, the case was reclassified as a cellular variant of ScRMS due to the presence of focal areas of sclerosis. This case raises the question of whether a subset of the so-called fusion-negative solid ARMS represents in fact cellular/solid-variants of ScRMS. Indeed a recent re-review of the ARMS in patients enrolled in the Children Oncology Group (COG)

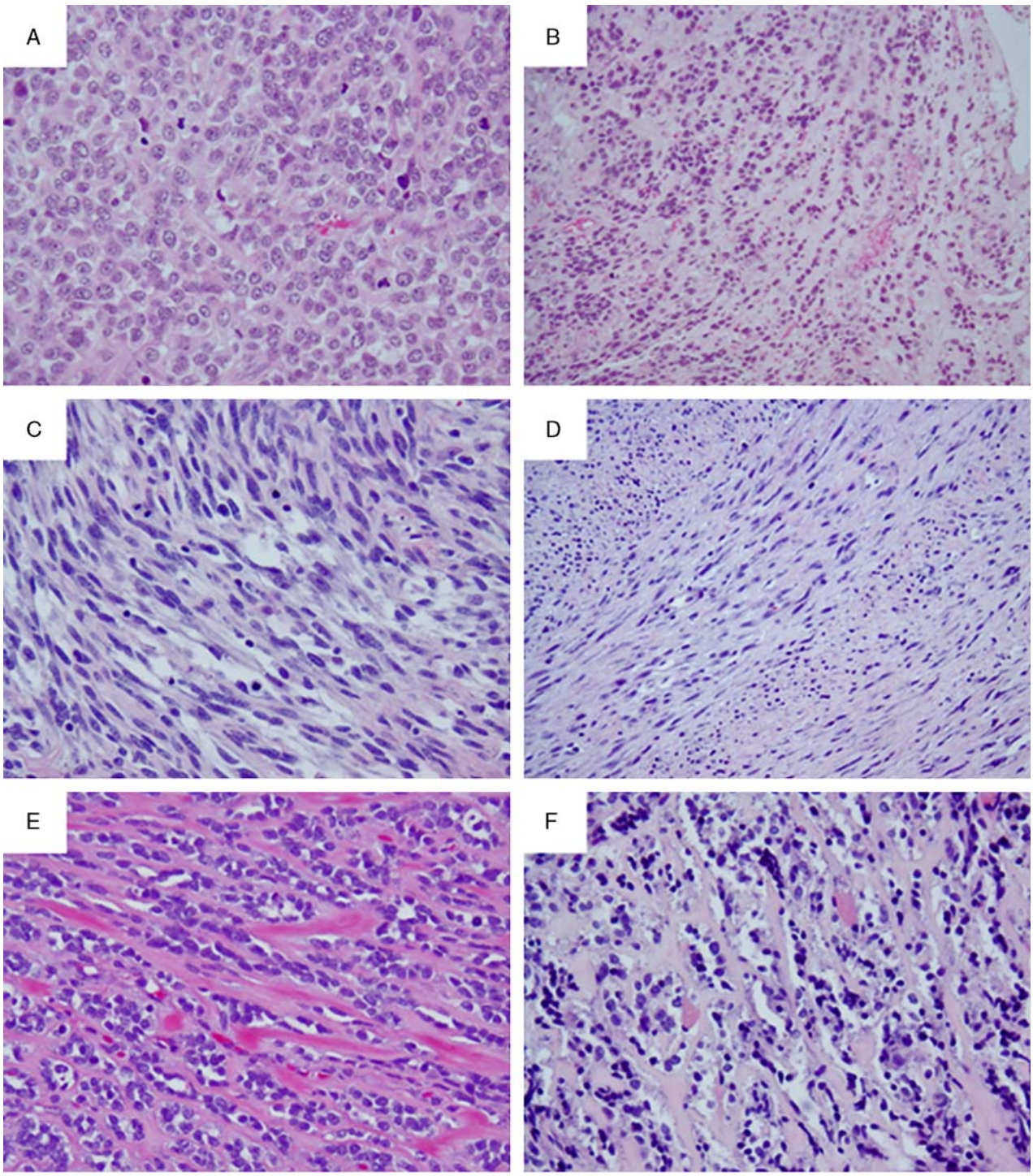

FIGURE 5. Wide morphologic spectrum of *MYOD1*-mutant pediatric SRMS. Coexisting *MYOD1*, *PIK3CA*, and *FGFR4* mutations were associated with a highly primitive and solid growth of undifferentiated round cells with high mitotic activity and necrosis (A; RMS17). Focal areas of dense sclerosis were noted in keeping with a cellular variant of ScRMS (B). *MYOD1*-mutant SRMSs from the head and neck area showing monomorphic spindle cells with fibrillary pale eosinophilic cytoplasm, fine chromatin, and scattered mitotic figures, in a loose edematous stroma (C, RMS20) or in a more sclerotic background and arranged in long sweeping fascicles (D, RMS21). Coexisting *MYOD1* and *PIK3CA* helical mutations in 2 ScRMSs showing a distinctive microalveolar growth pattern and alternating refractile collagen bundles (E, RMS15; F, RMS16).

studies from 1999 to 2005 resulted in the reclassification of 30% of cases, either into ERMS with a so-called "dense pattern" or ScRMS.[43] It also raises the possibility that accumulating secondary oncogenic mutations, possibly synergistic to the *MYOD1* initiating event, are responsible for blocking differentiation and associated fatal outcome. SRMS with *MYOD1* mutations showed significantly higher upregulation of *MYOD1* mRNA, on the basis of 2 cases with available RNAseq data, either occurring in an adult (adSRMS2) or in a child (SRMS17), compared with other RMS subtypes (Fig. 4).

Despite our detailed molecular investigation, there was a remaining third group of tumors, lacking recurrent genetic abnormalities and presenting with predilection in the genito-urinary or intra-abdominal location. Although the data are quite limited for definitive conclusions, these patients appeared to follow a more favorable course compared with the *MYOD1*-mutant cases and might either represent a third genetic group of SRMS or may be more closely related to the ERMS. Only 1 of these 5 cases showed *FGFR4 V550L* mutations, as previously documented in ERMS.[41]

In conclusion, despite a relatively similar histomorphology, pediatric SRMS is a heterogenous disease genetically as well as clinically. Our study identifies 3 distinct molecular subsets of SRMS/ScRMS within the pediatric age group. First, tumors presenting at birth or within 1 year of age occur with predilection in the trunk and are associated with recurrent gene fusions, involving critical transcriptional activators of muscle-specific genes, such as *VGLL2*, *TEAD1*, and *SRF*. Most importantly, these patients follow a favorable clinical outcome, lacking metastatic potential, all being alive and well at long-term follow-up. This fusion-positive infantile SRMS group appears closely reminiscent to the behavior of *ETV6-NTRK3*-positive infantile fibrosarcomas and militate against their classification as a "high-grade neoplasm." Second, our findings further show that pediatric *MYOD1*-mutant SRMSs, with or without accompanying *PIK3CA* mutations, follow a highly aggressive course with high mortality despite multimodality therapy. In fact, *MYOD1* mutation was the most common genetic abnormality in pediatric SRMS, occurring in 67% of children beyond 1 year of age, and can be used as a molecular diagnostic test to stratify these high-risk patients. Third, despite our detailed molecular investigation, there is a remaining group lacking gene fusions or *MYOD1* mutations often presenting intra-abdominally or in the genito-urinary area. This latter subset seems to follow a favorable clinical course; however, the data remain limited to determine whether it represents a separate molecular group or has a closer relationship to the more common ERMS in this location.

ACKNOWLEDGMENTS

The authors thank Milagros Soto for editorial assistance and the efforts of Agnès Viale and the Genomics Core Laboratory at MSKCC where RNA sequencing was performed.

REFERENCES

1. Missiaglia E, Williamson D, Chisholm J, et al. PAX3/FOXO1 fusion gene status is the key prognostic molecular marker in rhabdomyosarcoma and significantly improves current risk stratification. *J Clin Oncol*. 2012;30:1670–1677.
2. Carli M, Colombatti R, Oberlin O, et al. European intergroup studies (MMT4-89 and MMT4-91) on childhood metastatic rhabdomyosarcoma: final results and analysis of prognostic factors. *J Clin Oncol*. 2004;22:4787–4794.
3. Oberlin O, Rey A, Lyden E, et al. Prognostic factors in metastatic rhabdomyosarcomas: results of a pooled analysis from United States and European cooperative groups. *J Clin Oncol*. 2008;26:2384–2389.
4. Cavazzana AO, Schmidt D, Ninfo V, et al. Spindle cell rhabdomyosarcoma. A prognostically favorable variant of rhabdomyosarcoma. *Am J Surg Pathol*. 1992;16:229–235.
5. Leuschner I, Newton WA Jr, Schmidt D, et al. Spindle cell variants of embryonal rhabdomyosarcoma in the paratesticular region. A report of the Intergroup Rhabdomyosarcoma Study. *Am J Surg Pathol*. 1993;17:221–230.
6. Mentzel T, Katenkamp D. Sclerosing pseudovascular rhabdomyosarcoma in adults. Clinicopathological and immunohistochemical analysis of three cases. *Virchows Arch*. 2000;436:305–311.
7. Folpe AL, McKenney JK, Bridge JA, et al. Sclerosing rhabdomyosarcoma in adults: report of four cases of a hyalinizing, matrix-rich variant of rhabdomyosarcoma that may be confused with osteosarcoma, chondrosarcoma, or angiosarcoma. *Am J Surg Pathol*. 2002;26:1175–1183.
8. Mentzel T, Kuhnen C. Spindle cell rhabdomyosarcoma in adults: clinicopathological and immunohistochemical analysis of seven new cases. *Virchows Arch*. 2006;449:554–560.
9. Mentzel T. Spindle cell rhabdomyosarcoma in adults: a new entity in the spectrum of malignant mesenchymal tumors of soft tissues. *Pathologe*. 2010;31:91–96.
10. Fletcher C, Bridge JA, Hogendoorn PC, et al. *WHO Classification of Tumours of Soft Tissue and Bone*. Lyon: IARC; 2013.
11. Agaram NP, Chen CL, Zhang L, et al. Recurrent MYOD1 mutations in pediatric and adult sclerosing and spindle cell rhabdomyosarcomas: evidence for a common pathogenesis. *Genes Chromosomes Cancer*. 2014;53:779–787.
12. Mosquera JM, Sboner A, Zhang L, et al. Recurrent NCOA2 gene rearrangements in congenital/infantile spindle cell rhabdomyosarcoma. *Genes Chromosomes Cancer*. 2013;52:538–550.
13. Quail MA, Kozarewa I, Smith F, et al. A large genome center's improvements to the Illumina sequencing system. *Nature Methods*. 2008;5:1005–1010.
14. Dobin A, Davis CA, Schlesinger F, et al. STAR: ultrafast universal RNA-seq aligner. *Bioinformatics*. 2013;29:15–21.
15. Kim D, Pertea G, Trapnell C, et al. TopHat2: accurate alignment of transcriptomes in the presence of insertions, deletions and gene fusions. *Genome Biol*. 2013;14:R36.
16. Sboner A, Habegger L, Pflueger D, et al. FusionSeq: a modular framework for finding gene fusions by analyzing paired-end RNA-sequencing data. *Genome Biol*. 2010;11:R104.
17. Kim D, Salzberg SL. TopHat-Fusion: an algorithm for discovery of novel fusion transcripts. *Genome Biol*. 2011;12:R72.
18. Habegger L, Sboner A, Gianoulis TA, et al. RSEQtools: a modular framework to analyze RNA-Seq data using compact, anonymized data summaries. *Bioinformatics*. 2011;27:281–283.
19. Cibulskis K, Lawrence MS, Carter SL, Sivachenko A, Jaffe D, Sougnez C, Gabriel S, Meyerson M, Lander ES, Getz G. Sensitive detection of somatic point mutations in impure and heterogeneous cancer samples. *Nat Biotechnol*. 2013;31:213–9.
20. Koboldt DC, Zhang Q, Larson DE, Shen D, McLellan MD, Lin L, Miller CA, Mardis ER, Ding L, Wilson RK. VarScan 2: somatic mutation and copy number alteration discovery in cancer by exome sequencing. *Genome Res*. 2012;22:568–76.
21. Antonescu CR, Sommer G, Sarran L, Tschernyavsky SJ, Riedel E, Woodruff JM, Robson M, Maki R, Brennan MF, Ladanyi M, DeMatteo RP, Besmer P. Association of KIT exon 9 mutations with nongastric primary site and aggressive behavior: KIT mutation

analysis and clinical correlates of 120 gastrointestinal stromal tumors. *Clin Cancer Res*. 2003;9:3329–37.
22. Lundgren L, Angervall L, Stenman G, et al. Infantile rhabdomyofibrosarcoma: a high-grade sarcoma distinguishable from infantile fibrosarcoma and rhabdomyosarcoma. *Hum Pathol*. 1993;24:785–795.
23. Rubin BP, Hasserjian RP, Singer S, et al. Spindle cell rhabdomyosarcoma (so-called) in adults: report of two cases with emphasis on differential diagnosis. *Am J Surg Pathol*. 1998;22:459–464.
24. Nascimento AF, Fletcher CD. Spindle cell rhabdomyosarcoma in adults. *Am J Surg Pathol*. 2005;29:1106–1113.
25. Maeda T, Chapman DL, Stewart AF. Mammalian vestigial-like 2, a cofactor of TEF-1 and MEF2 transcription factors that promotes skeletal muscle differentiation. *J Biol Chem*. 2002;277:48889–48898.
26. Paumard-Rigal S, Zider A, Vaudin P, et al. Specific interactions between vestigial and scalloped are required to promote wing tissue proliferation in *Drosophila melanogaster*. *Dev Genes Evol*. 1998;208:440–446.
27. Vaudin P, Delanoue R, Davidson I, et al. TONDU (TDU), a novel human protein related to the product of vestigial (vg) gene of Drosophila melanogaster interacts with vertebrate TEF factors and substitutes for Vg function in wing formation. *Development*. 1999;126:4807–4816.
28. Yoshida T. MCAT elements and the TEF-1 family of transcription factors in muscle development and disease. *Arterioscler Thromb Vasc Biol*. 2008;28:8–17.
29. Kim J, Sebring A, Esch JJ, et al. Integration of positional signals and regulation of wing formation and identity by Drosophila vestigial gene. *Nature*. 1996;382:133–138.
30. Gunther S, Mielcarek M, Kruger M, et al. VITO-1 is an essential cofactor of TEF1-dependent muscle-specific gene regulation. *Nucleic Acids Res*. 2004;32:791–802.
31. Pipes GC, Creemers EE, Olson EN. The myocardin family of transcriptional coactivators: versatile regulators of cell growth, migration, and myogenesis. *Genes Dev*. 2006;20:1545–1556.
32. Qiu H, Wang F, Liu C, et al. TEAD1-dependent expression of the FoxO3a gene in mouse skeletal muscle. *BMC Mol Biol*. 2011;12:1.
33. Liu Y, Wang F, Wu Y, et al. Variations of CITED2 are associated with congenital heart disease (CHD) in Chinese population. *PLoS One*. 2014;9:e98157.
34. Xu M, Wu X, Li Y, et al. CITED2 mutation and methylation in children with congenital heart disease. *J Biomed Sci*. 2014;21:7.
35. Hofvander J, Tayebwa J, Nilsson J, et al. Recurrent PRDM10 gene fusions in undifferentiated pleomorphic sarcoma. *Clin Cancer Res*. 2015;21:864–869.
36. Chen D, Ma H, Hong H, et al. Regulation of transcription by a protein methyltransferase. *Science*. 1999;284:2174–2177.
37. Koh SS, Chen D, Lee YH, et al. Synergistic enhancement of nuclear receptor function by p160 coactivators and two coactivators with protein methyltransferase activities. *J Biol Chem*. 2001;276:1089–1098.
38. Szuhai K, de Jong D, Leung WY, et al. Transactivating mutation of the MYOD1 gene is a frequent event in adult spindle cell rhabdomyosarcoma. *J Pathol*. 2014;232:300–307.
39. Kohsaka S, Shukla N, Ameur N, et al. A recurrent neomorphic mutation in MYOD1 defines a clinically aggressive subset of embryonal rhabdomyosarcoma associated with PI3K-AKT pathway mutations. *Nat Genet*. 2014;46:595–600.
40. Shern JF, Chen L, Chmielecki J, et al. Comprehensive genomic analysis of rhabdomyosarcoma reveals a landscape of alterations affecting a common genetic axis in fusion-positive and fusion-negative tumors. *Cancer Discov*. 2014;4:216–231.
41. Taylor JGt, Cheuk AT, Tsang PS, et al. Identification of FGFR4-activating mutations in human rhabdomyosarcomas that promote metastasis in xenotransplanted models. *J Clin Invest*. 2009;119:3395–3407.
42. Shukla N, Ameur N, Yilmaz I, et al. Oncogene mutation profiling of pediatric solid tumors reveals significant subsets of embryonal rhabdomyosarcoma and neuroblastoma with mutated genes in growth signaling pathways. *Clin Cancer Res*. 2012;18:748–757.
43. Rudzinski ER, Anderson JR, Hawkins DS, et al. The World Health Organization Classification of skeletal muscle tumors in pediatric rhabdomyosarcoma: a report from the Children's Oncology Group. *Arch Pathol Lab Med*. 2015. [Epub ahead of print].